Computational analysis of PTP-1B site-directed mutations and their structural binding to potential inhibitors

Munazzah Tasleem[1], Ambreen Shoaib[2], Asma Al-Shammary[3,] Abdelmuhsin Abdelgadir[4,5], Zeina El Asmar[4], Qazi Mohammad Sajid Jamal[6], Abdulwahed Alrehaily[7], Fevzi Bardcki[4], Abdel Moneim E. Sulieman [4], Tarun Kumar Upadhyay[8], Irfan Ahmad Ansari[9], Dakun Lai[1], Riadh Badraoui[4,10], Dharmendra Kumar Yadav[11,*], Mohd Saeed[4*]

[1] School of Electronic Science and Engineering, University of Electronic Science and Technology of China, Chengdu 610054, Sichuan, China
[2] Department of Pharmacy Practice, College of Pharmacy, Jazan University, P. Box No. 114, Jazan, Saudi Arabia
[3] Department of Public Health, College of Public Health and Health Informatics, University of Ha'il, P.O. Box 2240, Ha'il 81451, Saudi Arabia
[4] Department of Biology, College of Sciences, University of Hail, PO Box 2240, Hail, KSA
[5] National Centre for Research, P.O. Box 1304, Khartoum, Sudan
[6] Department of Health Informatics, College of Public Health and Health Informatics, Qassim University, Al Bukayriyah, Saudi Arabia
[7] Department of Biology, Faculty of Science, Islamic University of Madinah, P.O. Box 170, Madinah 42351, Saudi Arabia
[8] Department of Biotechnology, Parul Institute of Applied Sciences and Animal Cell Culture and Immunobiochemistry Lab, Centre of Research for Development, Parul University, Vadodara 391760, India
[9] Department of Biosciences, Integral University, Lucknow, India
[10] Section of Histology-Cytology, Faculty of Medicine of Tunis, University of Tunis El Manar, 1007 La Rabta-Tunis, Tunisia
[11] College of Pharmacy, Gachon University of Medicine and Science, Yeonsu-gu, Incheon City, 21924, Korea

ARTICLE INFO	ABSTRACT
	Protein tyrosine phosphatase-1B (PTP-1B) is a well-known therapeutic target for diabetes and obesity as it suppresses insulin and leptin signaling. PTP-1B deletion or pharmacological suppression boosted glucose homeostasis and insulin signaling without altering hepatic fat storage. Inhibitors of PTP-1B may be useful in the treatment of type 2 diabetes, and shikonin, a naturally occurring naphthoquinone dye pigment, is reported to inhibit PTP-1B and possess antidiabetic properties. Since the cell contains a large number of phosphatases, PTP-1B inhibitors must be effective and selective. To explore more about the mechanism underlying the inhibitor's efficacy and selectivity, we investigated its top four pharmacophores and used site-directed mutagenesis to insert amino acid mutations into PTP-1B as an extension of our previous study where we identified 4 pharmacophores of shikonin. The study aimed to examine the site-directed mutations like R24Y, S215E, and S216C influence the binding of shikonin pharmacophores, which act as selective inhibitors of PTP-1B. To achieve this purpose, docking and molecular dynamics simulations of wild-type (WT) and mutant PTP-1B with antidiabetic compounds were undertaken. The simulation results revealed that site-directed mutations can change the hydrogen bond and hydrophobic interactions between shikonin pharmacophores and many residues in PTP-1B's active site, influencing the drug's binding affinity. These findings could aid researchers in better understanding PTP-1B inhibitors' selective binding mechanism and pave the path for the creation of effective PTP-1B inhibitors.

Introduction

The pathogenesis of a wide range of significant human disorders, including diabetes and obesity, has been linked to abnormal signal transduction pathways and the resulting disruption of normal protein phosphorylation patterns (1). For example, a selective capacity to target these pathways offers tremendous therapeutic potential. There has been a dramatic rise in the use of protein kinase inhibitors in recent years. Protein tyrosine kinase (PTK) based medication development has run across several obstacles, such as resistance to several medicines. As a result, there

is an urgent demand for identifying novel targets and techniques. Since protein phosphorylation is a reversible process, it is important to remember that the coordinated and competing actions of the two types of enzymes involved in protein phosphorylation are critical to signaling outcomes. The protein tyrosine phosphatases (PTPs), which are a vast family of proteins that operate in conjunction with PTKs to modulate cell signaling, have also been implicated in the etiology of several human disorders, including diabetes and Alzheimer's disease (2). PTPs remain primarily unexploited as therapeutic targets. In the insulin and leptin signaling pathways, PTP-1B plays a critical role in the

dephosphorylation of insulin and leptin receptors (3, 4). According to several research studies, PTP-1B-knockout mice have enhanced insulin sensitivity and are resistant to diet-induced obesity, whereas therapy with PTP-1B antisense oligonucleotides improves hyperglycemia in diabetic mice models (5, 6). Therefore, PTP-1B, the prototypic PTP, is a recognized target for the treatment of diabetes and obesity because it plays a well-established function in downregulating insulin and leptin signaling (7). Additionally, several studies revealed the importance of genetic deletion or pharmacological suppression of PTP-1B in improving glucose homeostasis and insulin signaling without generating fat accumulation in the liver, which proved to be advantageous over existing therapies (8).

Saeed M. et al. showed the binding of potent natural antidiabetic compounds shikonin and its pharmacophores (ZINC000031168045, ZINC000031168048, ZINC000031168041, and ZINC000031168554) with the active site residues within the binding pocket of PTP-1B. These compounds were observed to form hydrogen bonds with the active site residues (ARG24, SER215, SER216, ARG221, and ARG254) in the binding pocket of PTP-1B to stabilize the structure (9). Various PTP-1B inhibitors have been successfully found, including pTyr mimetics and natural products; however, the catalytic domain of PTP-1B, which is highly conserved, makes it difficult to increase the inhibitor's selectivity over other PTPs (10). Furthermore, to design potent inhibitors, active site residues can be explored by site-directed mutagenesis.

To gain a better understanding of the structural basis for PTP-1B recognition of inhibitors and to establish the basis for the subsequent design of specific compounds capable of interfering with PTP-1B-related processes, we must first characterize the regions that comprise the inhibitor binding sites (the previously identified active site residues) and understand the basis of the potency and selectivity of shikonin. Therefore, the objective of this study was to investigate the rationale of shikonin's efficacy and selectivity by analyzing its top four pharmacophores (9) and by introducing amino acid mutations into PTP-1B by site-directed mutagenesis. To execute this study by employing *in silico* technique, we used site-directed mutagenesis, molecular docking, and molecular dynamics (MD) simulations to examine the internal behaviors of the PTP-1B-inhibitor complex and mutant complex. The conformational changes, in-tra-molecular interactions, and energy differences of shikonin and its pharmacophores were analyzed to gain a better understanding of the key elements impacting binding selectivity. In light of the above, this study explored the binding mode of shikonin and its top pharmacophores with PTP1B via introducing amino acid substitution into the active site residues to uncover novel implications for the design of PTP-1B inhibitors that are both potent and selective.

Materials and Methods

Data retrieval

Structural and sequence data of PTP-1B was downloaded from PDB (Protein Data Bank), a database of experimentally (NMR or X-Ray crystallography) determined three-dimensional structures of the protein (11, 21). PDB ID: 1AAX _A resolution1.9Å was downloaded along with its FASTA sequence. 1AAX contains a single A chain with 321 amino acids forming compact alpha helices and beta sheets. The structure is bound to 4-PHOSPHONOOXY-PHENYL-METHYL-[4-PHOSPHONOOXY] BENZEN (BPM) in its binding pocket.

Orthologous analysis

PTP-1B is described as a negative regulator of insulin and leptin signaling and a modulator of various processes in the central nervous system (CNS). The sequence data from different species of PTP-1B was collected to identify the conserved and nonconserved amino acids. PTP-1B FASTA sequence retrieved from PDB was searched using BLAST-P (12, 27) for obtaining orthologous; the search was constrained to mammals only. The sequence alignment and construction of the phylogenetic tree were carried out with the help of MEGA X. The Maximum Likelihood approach and the Poisson correction model with 1000 bootstrap methods were used to infer the evolutionary history of the organism.

Multiple sequence alignment

Aligning the sequences of orthologous gives insight into conserved and nonconserved amino acid sites. The Clustal Omega program was used for PTP-1B Orthologous multiple sequence alignment (13, 11). The program works with the progressive alignment method and aligns the sequences globally by meeting a pairwise alignment consensus.

Mutation analysis

For each of the active site residues of 1AAX, the impact of single-point mutations on protein stability was assessed. Therefore, the mutation energy for each active site residue was calculated by applying CHARMm Polar H force field at pH7.4 by using the 'calculated Mutation Energy' protocol from DS. This tool scans for amino acid residues and mutates them to one or even more specified amino acid types. The difference in the free energy of folding between the mutant structure and the wild-type protein is used to determine the energy effect of each mutation on protein stability.

Modeling of PTP-1B mutants

The most stable and favorable mutations in the conserved positions were manually introduced into the wild PTP-1B sequence. The mutant variants were modeled using the 'Build Mutant' protocol from DS. The modeled structure was minimized by applying the CHARMm force field.

Docking analysis

Shikonin (ZINC000002015152), ZINC000031168045, ZINC000031168048, ZINC000031168041, and ZINC000031168554 were docked into the binding pocket of PTP-1B using CDOCKER protocol from DS. Mutant model structures were prepared using the 'prepared Protein' protocol from DS. BPM was removed from the binding pocket of PTP-1B structure, and a binding site sphere of radius 15.50 Å centered at 44.5652, 12.7344, 0.703289, in x, y, and z directions was generated by the 'Define Site' protocol from DS. Docking was carried out by applying the CHARMm force field for generating random conformations by deploying 1000 dynamic steps and simulated annealing. The receptor was kept rigid during the refining process while the ligands were enabled flexibly. The best

confirmation of the antidiabetic compounds was selected based on the highest CDOCKER energy.

Assessment of complex stability

The binding energy of the selected poses was computed by the 'Calculate Binding Energy' Protocol in DS. Ligand van der Waals clashes were removed by performing In Situ Ligand Minimization to calculate the binding energy. The equation for determining the binding energy is as follows:

Energy Binding = Energy Complex - Energy Ligand - Energy Receptor

Comparative intra-molecular interaction studies

Close intramolecular interactions of shikonin, ZINC000031168045, ZINC000031168048, ZINC000031168041, and ZINC000031168554 within the binding site residues of the mutant models were analyzed. Intra-molecular interactions of the identified antidiabetic compounds (9) and wild-type PTP-1B were compared with the interactions formed between mutant models and shikonin to assess the role of mutation instability.

Molecular Dynamics (MD) simulations

Molecular dynamics (MD) simulations were performed by Desmond version 5.3 with an inbuilt OPLS3 force field. Dynamic simulations were carried out by choosing selected docking poses for molecular docking. Detailed procedures were described by Tiwari et al.. (14, 28). The binding free energy (MM-GBSA) was also calculated from the last 5 ns of the ligand-protein dynamic simulation trajectory (15, 28).

Results

Orthologous analysis

Orthologs from seventeen species possessing sequence similarities within the range of 97-99% with 100% query coverage were selected for this study. The phylogenetic tree was scaled in branch length units corresponding to the evolutionary distance. The Maximum Likelihood technique was used for calculating evolutionary distances in the number of base substitutions per site unit, describing 1AAX closest to XP011721170.1. The phylogenetic tree was initially divided into two major clusters. The first cluster was further divided into four clusters (C1 to C4) based on the evolutionary distance, as shown in Figure 1.

Multiple sequence alignment

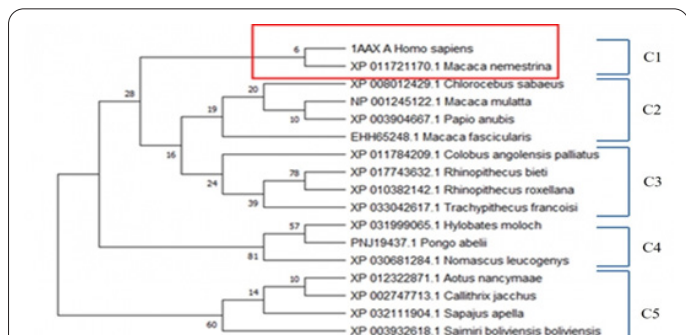PTP-1B ortholog sequences of 17 selected species were

Figure 1. Poisson correction model and the Maximum Likelihood approach were used to estimate the evolutionary history. Seventeen orthologous sequences were examined.
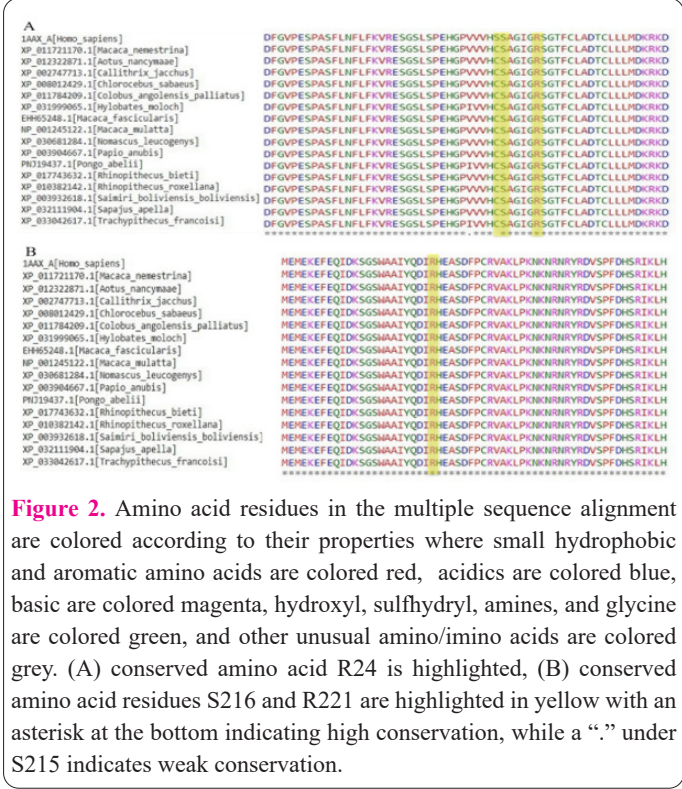

Figure 2. Amino acid residues in the multiple sequence alignment are colored according to their properties where small hydrophobic and aromatic amino acids are colored red, acidics are colored blue, basic are colored magenta, hydroxyl, sulfhydryl, amines, and glycine are colored green, and other unusual amino/imino acids are colored grey. (A) conserved amino acid R24 is highlighted, (B) conserved amino acid residues S216 and R221 are highlighted in yellow with an asterisk at the bottom indicating high conservation, while a "." under S215 indicates weak conservation.
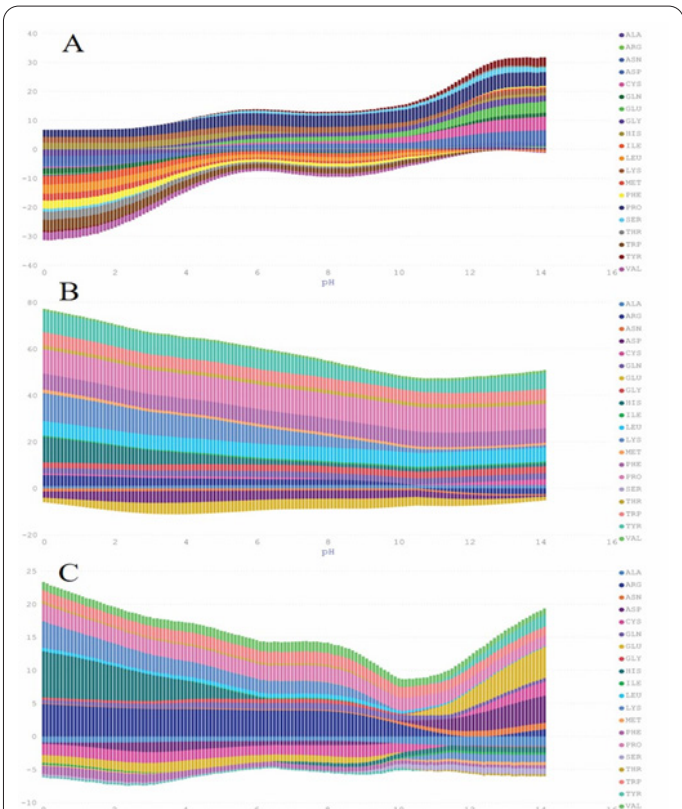

Figure 3. Computed mutation energy of Arg24 (A), Ser215 (B), and Ser216(C) at pH interval range from 0-14.

aligned by employing Clustal Omega multiple sequence alignment tool (13,11). The alignment revealed conserved and nonconserved amino acid positions, as shown in Figure 2 (16,12).

Prediction of favorable and stabilizing mutations

Mutation scanning for active site residues forming hydrogen bonds with shikonin (Arg24, Ser215, Ser216, Arg221, and Arg254) was carried out using the 'calculated Mutation Energy' protocol from Biovia Discovery Studio

(DS) [Dassault Systems, BIOVIA Corp., San Diego, CA, USA, v 21.1]. Arg24, when mutated to Trp, Leu, Ilu, Val, and Phe, resulted in a stabilized structure; the mutant Trp had the highest stability with mutation energy of -1.49 kcal/mol at pH 7.4, as shown in Table S1. Mutation energy calculated for all mutant amino acids at pH intervals from 0-14 is shown in Figure 3 A.

The mutation energy of Ser215 was estimated at different pH levels with other amino acids, as shown in Figure 3B. When Ser215 was changed to Glu, Asp, and Asn, the structure was stabilized, with the mutant Glu having the highest stability at -4.38 kcal/mol, as shown in Table S2. Figure 3C depicts the Ser216 mutation energy at various pH levels compared to other amino acids. Mutant CYS had the best stability at -1.49 kcal/mol when SER216 was replaced by CYS, GLU, PHE, ALA, and ASP, as shown in Table S3. The active site residues Arg221 and Arg254 could not be stabilized by any mutants, as shown in Tables S4 and S5. The generated mutant model and the wild-type mutant model were aligned together to discern structural deviations, as shown in Figure 4.

Stability assessment and comparative intra-molecular interaction studies.

The free binding energy of shikonin and wild-type PTP-1B was observed to be -87.8102 kcal/mol, as shown in Table 1. Selected top pharmacophores from our previous study (9), when docked within the binding pocket of the PTP-1B mutant R24Y, show free binding energy within the range of -57.04 to -104.28 kcal/mol, as shown in Table 2 and Figure 5. Essential intramolecular interactions are formed between shikonin and mutant R24Y PTP-1B, assisting in the binding of the ligand, as shown in Figure 6.

The free binding energy of PTP-1B mutant S215E ranges from -134.04 to -183.52 kcal/mol, as shown in Table 3. It was found that ZINC000031168048 had the lowest free binding energy of the entire selected antidiabetic compound, indicating a high binding affinity of the compound in the PTP-1B binding pocket. Compound ZINC000031168045 and shikonin were observed to form hydrogen bonds with the mutant residue Glu215.

Computed for PTP-1B mutant S216C ranges from -121.16 to -187.06 kcal/mol, as shown in Table 4. Compound ZINC000031168041 shows the lowest binding energy. All compounds are involved in forming pi interactions with the PTP-1B mutant S216C. Pi interactions feature various binding confirmations including pi-sigma, pi-cation, and pi-pi (17). The mutant residue Csy216 forms pi-sulfur interactions with shikonin. All of the selected pharmacophores and their interactions with the active site residues of the mutant models are shown in Figure S1-S12.

Molecular dynamics simulations

The protein-ligand complex stability was evaluated by measuring the root-mean-square deviation (RMSD) and root mean square fluctuations (RMSFs) to determine the fluctuation/thermal motion in protein residues during the simulation. The RMSD plots of shikonin for R24Y, S215E, S216C, and WT PTP-1B are shown in Figures 7 and 8 and gives an overview of protein conformational perturbation during the binding. The RMSD analysis shows a higher RMSD of shikonin for mutant R24Y, S215E, and S216C compared to WT PTP-1B. The RMSD plot of WT PTP-1B revealed that, after 10 ns, the shikonin system attains the
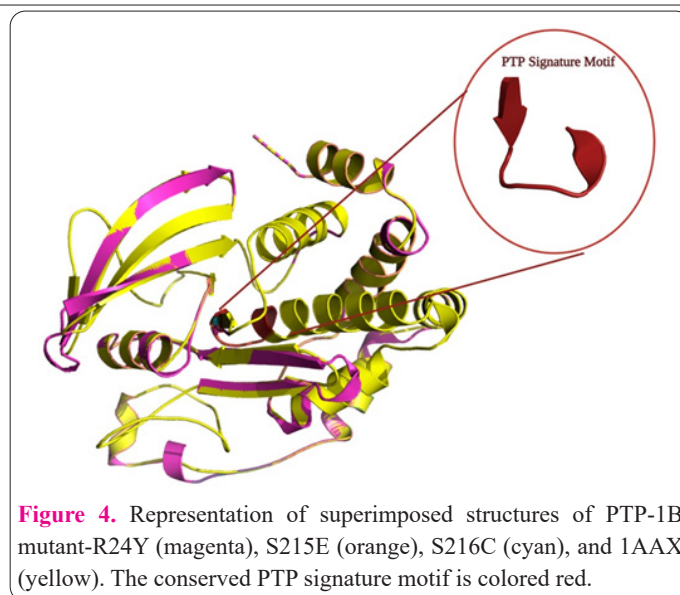

Figure 4. Representation of superimposed structures of PTP-1B mutant-R24Y (magenta), S215E (orange), S216C (cyan), and 1AAX (yellow). The conserved PTP signature motif is colored red.
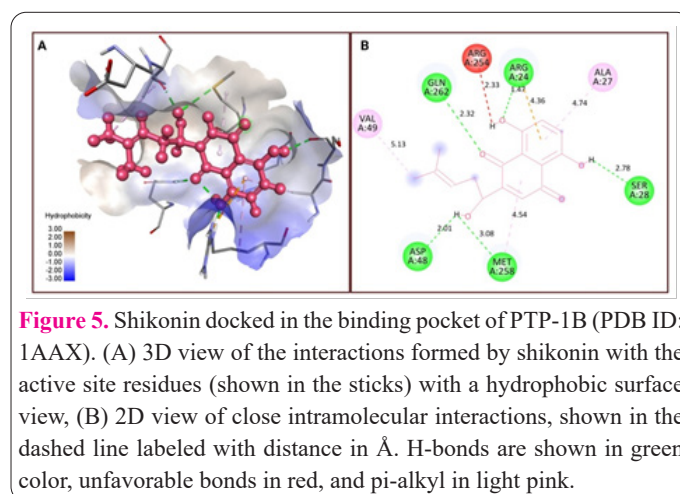

Figure 5. Shikonin docked in the binding pocket of PTP-1B (PDB ID: 1AAX). (A) 3D view of the interactions formed by shikonin with the active site residues (shown in the sticks) with a hydrophobic surface view, (B) 2D view of close intramolecular interactions, shown in the dashed line labeled with distance in Å. H-bonds are shown in green color, unfavorable bonds in red, and pi-alkyl in light pink.
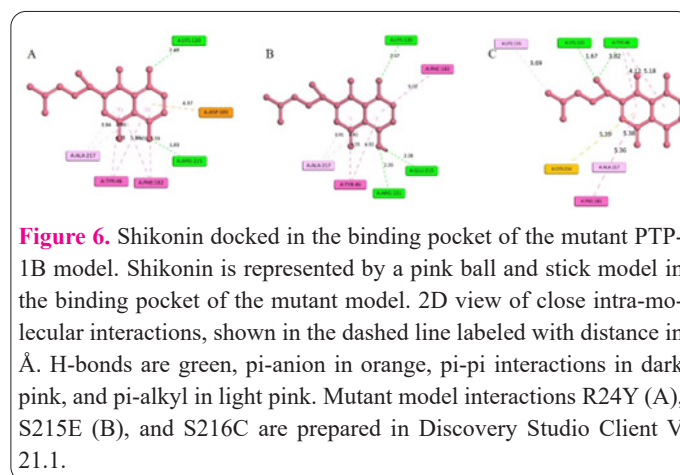

Figure 6. Shikonin docked in the binding pocket of the mutant PTP-1B model. Shikonin is represented by a pink ball and stick model in the binding pocket of the mutant model. 2D view of close intra-molecular interactions, shown in the dashed line labeled with distance in Å. H-bonds are green, pi-anion in orange, pi-pi interactions in dark pink, and pi-alkyl in light pink. Mutant model interactions R24Y (A), S215E (B), and S216C are prepared in Discovery Studio Client V 21.1.
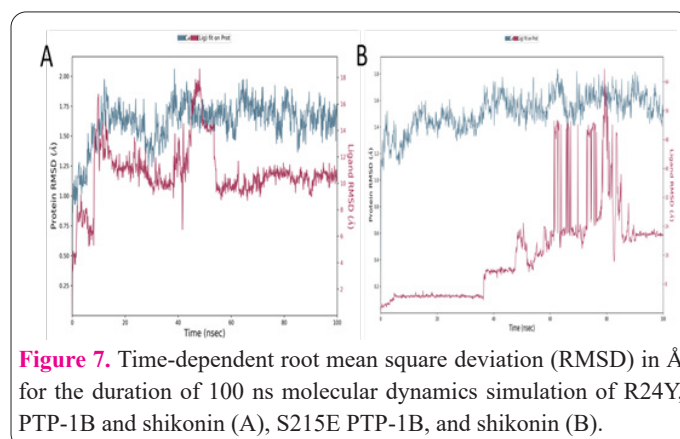

Figure 7. Time-dependent root mean square deviation (RMSD) in Å for the duration of 100 ns molecular dynamics simulation of R24Y, PTP-1B and shikonin (A), S215E PTP-1B, and shikonin (B).

Table 1. Intra-molecular interactions formed between the wild type PTP-1B (PDB ID: 1AAX) and shikonin pharmacophores.

Compound	Wild type PTP-1B Intra-molecular Interactions	Binding Energy	CDOCKER Energy
ZINC000002015152	H-bond (Conventional): Arg24, Gln262, Asp48, Met258, Ser28. Pi-Cation: Arg24. Alkyl: Val49. Pi-Alkyl: Met258, Arg24, Ala27.	-87.8102	-5.42405
ZINC000031168554	H-bond (Conventional): Lys120, Ser216, Arg221, Gln266. H-bond (Carbon Hydrogen): Ser215. Pi-Sigma: Phe182.	-64.4451	19.1819
ZINC000031168041	H-bond (Conventional): Ser215, Ser216, Ala217, Gly218, Ile219, Gly220, Arg221, Arg254. H-bond (Carbon Hydrogen): Arg24, Ser215, Ser216, Glln262.	-207.255	-15.9035
ZINC000031168045	H-bond (Conventional): ARg24, Phe182, Ser215, Ser216, Ala217, Gly220, Arg221, Arg254, Gln266. H-bond (Carbon Hydrogen): Ser215, Ser216, Gly220. Pi-Sigma: Met258, Phe182. Pi-Sulfur: Met258.	-205.233	-20.083
ZINC000031168048	H-bond (Conventional): Arg24, Phe182, Ser215, Ala217, Gly218, Ile219, Arg221, Arg254, Gln266. H-bond (Carbon Hydrogen): Asp181, Ser215, Arg24. Pi-Sigma: Met258, Phe182.	-198.86	-15.2048

Table 2. Intra-molecular interactions formed between the PTP-1B mutant R24Y model and shikonin pharmacophores.

Compound	Mutant PTP-1B R24Y Intra-molecular Interactions	Binding Energy	CDOCKER Energy
ZINC000002015152	H-bond (Conventional): Lys120, Arg221. Pi Anion: Asp181. Pi-Pi stacked: Tyr46. Pi-Pi T-shaped: Phe182. Pi-Alkyl: Ala217.	-104.289	5.9615
ZINC000031168554	H-bond (Conventional): Arg221. H-bond (Carbon Hydrogen): Ser216. Pi-Pi stacked: Tyr46. Pi-Pi T-shaped: Phe182. Alkyl: Arg221 Pi-Alkyl: Phe182, Ala217.	-93.4955	28.766
ZINC000031168041	H-bond (Conventional): Tyr46, Gly220, Arg221. H-bond (Carbon Hydrogen): Gly220, Gln262. Pi-Pi stacked: Tyr46. Pi-Alkyl: Phe182, Ala217.	-88.2014	-15.4487
ZINC000031168045	H-bond (Conventional): Lys120. H-bond (Carbon Hydrogen): Gln262. Pi-Pi stacked: Tyr46. Pi-Alkyl: Trp24, Phe182, Aly217.	-68.0679	-24.0141
ZINC000031168048	H-bond (Conventional): Lys120, Arg22, Gln262. H-bond (Carbeon Hydrogen): Ser215, Ser216, Gln262. Pi-Pi Stacked: Tyr46. Pi-Pi T-shaped: Phe182. Alkyl: Val49. Pi-Alkyl: Phe182, Ala217.	-57.0428	-13.0523

Table 3. Intra-molecular interactions formed between the PTP-1B mutant S215E model and shikonin pharmacophores.

Compound	Mutant PTP-1B S215E Intra-molecular Interactions	Binding Energy	CDOCKER Energy
ZINC000031168048	H-bond (Conventional): Lys120. H-bond (Carbon Hydrogen): Lys120. Pi- Pi Stacked: Tyr46. Pi-Alkyl: Tyr46, Ala217.	-183.522	-16.2907
ZINC000031168041	H-bond (Conventional): Tyr20, Arg24, Lys120, Arg254, Asp48, Ser118. H-bond (Carbon Hydrogen): Arg24, Gln262. Pi-Sulfur: Met258. Alkyl: Ala217, Val49. Pi-Alkyl: Tyr46, Phe182.	-174.388	-17.4558
ZINC000031168045	H-bond (Conventional): Lys120, Glu215. H-bond (Carbon Hydrogen): Lys120. Pi-Alkyl: Ala217.	-173.66	-18.849
ZINC000002015152	H-bond (Conventional): Lys120, Arg221, Glu215. Pi-Pi Stacked: Tyr46. Pi-Pi T-shaped: Phe182. Pi-Alkyl: Ala217.	-145.836	3.53172
ZINC000031168554	H-bond (Conventional): Tyr46, Lys120, Ser216, Arg221. Pi-Pi Stacked: Tyr46. Pi-Pi T-shaped: Phe182. Pi-Alkyl: Ala217.	-134.044	28.9757

Table 4. Intra-molecular interactions formed between the PTP-1B mutant S216C model and shikonin pharmacophores.

| Compound	Mutant PTP-1B S216C Intra-molecular Interactions	Binding Energy	CDOCKER Energy
ZINC000031168041	H-bond (Conventional): Tyr20, Lys120, Arg254, Gln262. H-bond (Carbon Hydrogen): Arg24. Alkyl: Phe182.	-187.062	-15.0248
ZINC000031168048	H-bond (Conventional): Lys120, Gln262, Asp48. Alkyl: Val49, Ile219. Pi-Alkyl: Ty46, Lys116.	-150.072	-26.0043
ZINC000002015152	H-bond (Conventional): Tyr46, Lys120. Pi-Sulfur: Cys216. Pi-Pi Stacked: Tyr46. Alkyl: Lys116. Pi-Alkyl: Ala217.	-145.206	-0.473724
ZINC000031168554	H-bond (Conventional): Tyr46. Pi-Pi Stacked: Tyr46. Pi- Alkyl: Phe182, Ala217.	-134.99	23.0065
ZINC000031168045	H-bond (Conventional): Arg47, Lys120, Ser118. H-bond (Carbon Hydrogen): Tyr46. Pi-Anion: Asp48. Alkyl: Val49. Pi-Alkyl: Tyr46, Arg47.	-121.16	-31.3908
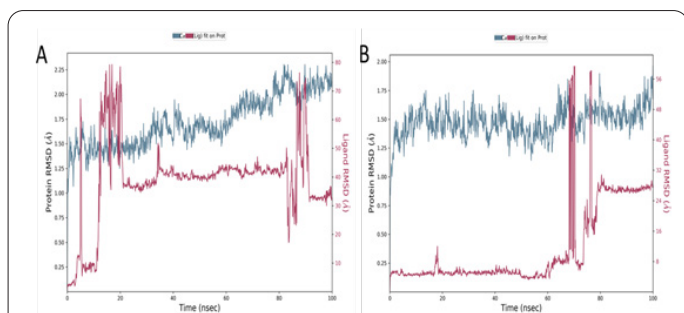
Figure 8. Time-dependent root mean square deviation (RMSD) in Å for the duration of 100 ns molecular dynamics simulation of S216C, PTP-1B, and shikonin (A), wild type (WT) PTP-1B (B).
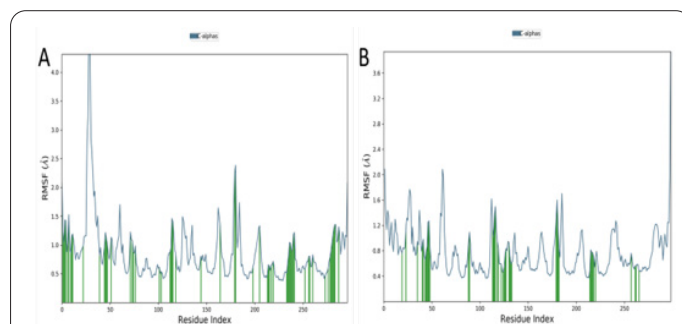

Figure 10. Root mean square fluctuations of Cα atoms during the 100 ns molecular dynamics simulation. The ligand contacts with protein residues are marked with green-colored vertical bars. S216C, PTP-1B and shikonin (A), wild type (WT) PTP-1B (B).
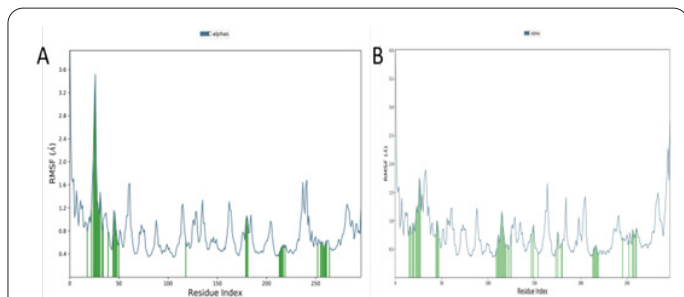

Figure 9. Root mean square fluctuations of Cα atoms during the 100 ns molecular dynamics simulation. Green vertical bars indicate ligand interactions with protein residues. R24Y PTP-1B and shikonin (A), S215E PTP-1B and shikonin (B).

equilibrium and then oscillates further with an RMSD of 1.0 Å and 2.0 Å, respectively. Whereas, mutant S216C models could not reach the equilibration. The fluctuations in mutant protein residues were analyzed by backbone atom motion and local changes in secondary structure elements. The RMSF for WT and mutant PTP-1B with shikonin are shown in Figures 9 and 10. The RMSF plot shows larger fluctuations in mutant models R24Y and S216C. The hydrogen bond interactions of shikonin and PTP-1B structures were evaluated. Hydrogen bond interaction with the mutant residue R24Y was not observed; however, hydrophobic interactions and water bridges were found during the trajectory. In addition, insignificant hydrogen bond formation was observed in S215E and S216C compared to the WT PTP-1B, as shown in Figure 11. We have further calculated before/after the average free energy of binding for PTP-1B inhibitor shikonin and the result is shown in Tables 5 and 6.

Discussion

The aim of the current study was to extend our previous work and explore the importance of the identified active site residues of PTP1B in binding to shikonin and its pharmacophores (9). Site-directed mutagenesis was used to
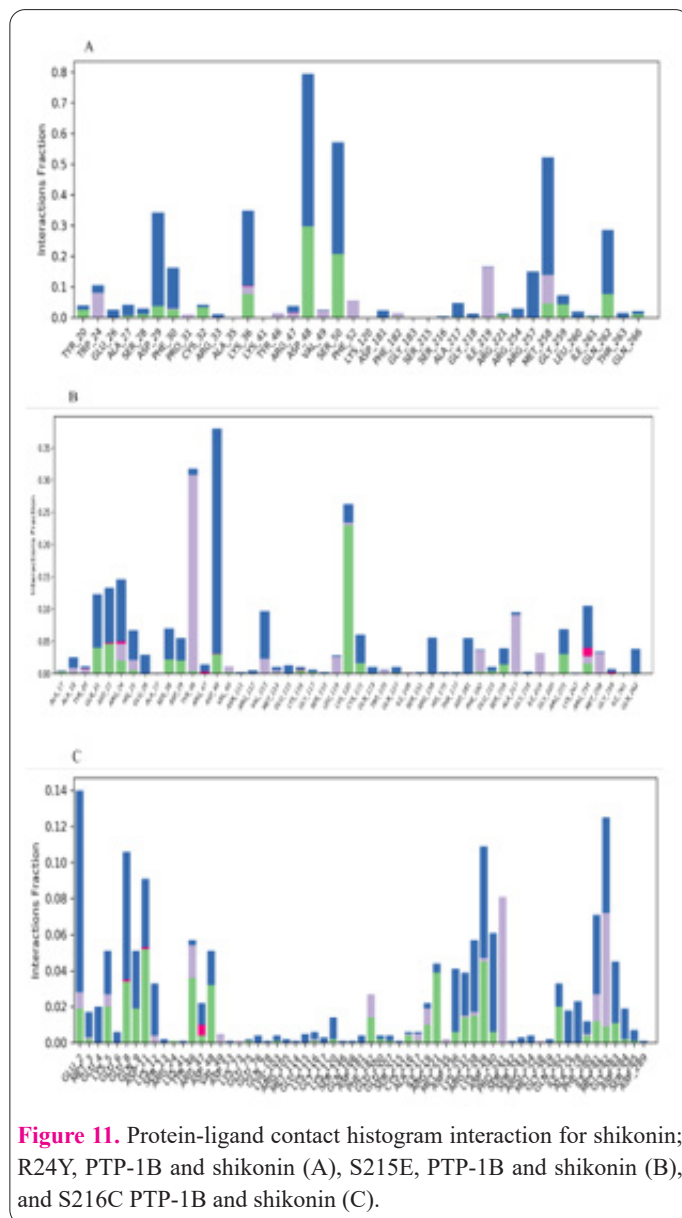

Figure 11. Protein-ligand contact histogram interaction for shikonin; R24Y, PTP-1B and shikonin (A), S215E, PTP-1B and shikonin (B), and S216C PTP-1B and shikonin (C).

Table 5. MM-GBSA binding free energy (before MD) and the corresponding energetic components of Shikonincomplex with the WT and Mutant protein (kcal/mol).

CMPD-ID	dG (Bind)	dG (Coulomb)	dG (Covalent)	dG (Hbond)	dG (Lipo)	dG (Solv_GB)	dG (vdW)
WT PTP-1B	-36.175	-7.452	2.752	-2.662	-15.396	21.42	-31.957
R24Y	-42.407	-21.588	1.504	-2.193	-14.591	27.417	-31.167
S215E	-41.371	-15.192	1.228	-2.43	-14.252	22.32	-31.199
S216C	-36.915	-14.707	0.558	-1.255	-11.449	17.031	-25.504

Table 6. MM-GBSA binding free energy (MD) and the corresponding energetic components of Shikonin complex with the WT and Mutant protein (kcal/mol).

CMPD-ID	dG (Bind)	dG (Coulomb)	dG (Covalent)	dG (Hbond)	dG (Lipo)	dG (Solv_GB)	dG (vdW)
WT PTP-1B	-26.55	-3.195	0.508	-1.292	-6.108	6.446	-22.908
R24Y	-39.221	-8.126	0.829	-0.588	-13.726	14.748	-32.298
S215E	-29.872	-7.132	0.424	-0.129	-11.178	18.548	-29.566
S216C	-11.109	-1.986	-0.072	-0.01	-1.2	5.608	-13.447

create a different mutant of PTP1B and their binding with shikonin and its identified pharmacophores to assess the effect of mutation on the binding of inhibitors of PTP1B.

Phylogenetic studies conducted on PTP-1B and its orthologous sequences of 17 species revealed a close association with Macaca nemestrina (accession no.: XP_011721170.1). The multiple sequence alignment reported a high similarity among the orthologs, where conserved amino acids are presented with '*' (asterisk) and nonconserved with a ':' (colon) at the bottom of the alignment (16, 18). The amino acid residues forming stable hydrogen bonds with shikonin pharmacophores, as presented in the study conducted by Saeed M et al. were selected to assess the selective binding of the active site residues, which are found to form stable hydrogen bonds in our previous study. The active site residues Arg24, Ser216, Arg221, and Arg254, were found highly conserved. At the same time, Ser215 indicates conservation between groups of amino acid residues sharing weakly similar properties by deploying the MSA technique.

Arg221 is an essential amino acid residue that forms a PTP signature motif in PTP-1B to induce catalysis (9). When Arg221 and Arg254 were mutated to any other residue, it resulted in an unstable mutation effect. Our observations revealed that Arg221 and Arg254 are intolerant to mutation. Generated mutant models: R24Y, S215E, and S216C were compared with wild-type structures of PTP-1B for any structural deviation. All three generated mutant models were observed to possess high similarity with the PTP-1B structure with a root mean square deviation (RMSD) value of 0.0 Å, as shown in Figure 6. No conformational change in the mutant model signifies its biological activity (19-22). A combination of evolutionary, intra-molecular interactions and mutational approaches were applied to explore amino acid residues with the tendency to mutate. Furthermore, all positions were examined structurally and energetically for favorable and stable mutations. Since the therapeutic drug effect depends on the target protein's structural stability, the goal was to discover readily mutable positions and residues that may prove to be structurally stable (21). Active site information obtained from the PTP-1B crystal structure (PDB ID-1AAX) revealed the amino acid composition of the binding pocket that includes Arg24, Tyr46, Asp48, Val49, Phe182, Ser215, Ser216, Ala217, Lys218, Ile219, Gly220, Arg221, Arg254, Gly259, and Gln262. The catalytically essential residues Cys and Arg are located in a conserved motif of the PTP signature motif (I/V)HCXAGXGR(S/T) lying in the binding pocket of PTP-1B, forming a portion of β-sheet, a loop, and a turn of α-helix.

The top four pharmacophores and shikonin were docked in the binding pocket of PTP-1B. Among the selected compounds, shikonin possessed the lowest free binding energy of -104.289 kcal/mol, indicating the highest binding affinity (16). In biological complexes, hydrogen bonds are the most common directed intermolecular interactions and are crucial in determining molecular recognition specificity. Shikonin was observed to form conventional hydrogen bonds with Lys120 and Arg221, where Arg221 is a conserved residue lying in the PTP signature motif. Drug–receptor interactions are primarily driven by hydrophobic interactions. Aromatic rings (benzene moiety and cyclic diketone) in shikonin were observed to form hydrophobic interactions with the active site residues. Aromatic ring interactions have a significant role in protein-ligand affinity and, consequently, drug design (23). These hydrophobic interactions formed within the wild-type (WT) PTP-1B and shikonin include pi-anion, pi-pi stacked, pi-pi T-shaped, and pi-alkyl that significantly add to the biological activity and stability of the protein-ligand complex. The pi-stacking interaction strengthens the binding affinity of the inhibitor to its target. However, other selected compounds were found to lose several hydrogen bonds, carbon-hydrogen bonds, and hydrophobic interactions with the active site residues, when bound with R24Y mutant PTP-1B, indicating a decrease in the stability and binding affinity. Carbon-hydrogen bonds are weak hydrogen bonds and are considered secondary interactions as bifurcated N–HO hydrogen bonds usually follow them. These bonds play a critical role in molecular recognition, protein folding, stability, nucleic acid-protein interaction, enzyme catalysis, and the stability of protein-ligand complexes (18, 24). It was observed that WT PTP-1B and selected com-pound complexes exhibit more hydrogen bonds than hydrophobic interactions.

PTP-1B mutant S215E docking with shikonin and ZINC000031168554 showed higher binding energy than with WT PTP-1B. Few compounds showed the formation of stable hydrogen bonds with the mutant residue (Gln215) of PTP-1B mutant S215E; however, many hydrogen bonds responsible for the formation of a stable complex were lost. Such as, ZINC000031168048 loses several intramolecular interactions although it forms a conventional hydrogen bond with the conserved residue Arg221 and few hydrophobic interactions. The complex of PTP-1B mutant S215E and ZINC000031168041 also revealed lesser stable intramolecular interactions with the active site residues; however, Met258 was found to form pi-sulfur interactions with ZINC000031168041. Although methionine is a hydrophobic residue, it stabilizes energy (25). Tyr46 was shown to form pi-stacking interactions with shikonin, ZINC000031168048, and ZINC000031168554, indicating a potential to improve the binding affinity of the inhibitor for its target (11, 22).

All selected compounds were observed to significantly lose stable hydrogen bonds and pi interactions with PTP-1B mutant S216C. Pi-interactions are unaffected by solvation/desolvation, they contribute to inhibitor binding. As a result, the penalties for enthalpy/entropy on free binding energy may be insignificant. Additionally, the reco-

gnition and organization of biomolecular structures rely on pi-pi stacking. Pi-sulfur interactions are reported to be responsible for the additional stabilizing energy associated with the binding affinity of the drug (27, 33). Stable hydrogen bonds were observed to form between the compounds (ZINC000031168554, ZINC000031168041, and ZINC000031168045) and WT PTP-1B, which did not exist when the compounds were docked with PTP-1B mutant S216C; however, despite losing several intra-molecular interactions, shikonin formed pi-sulfur interaction with the mutant residue Cys216.

In WT PTP-1B, the catalytic residue Arg221 lying in the PTP signature motif was noticed to form hydrogen bonds stabilizing the structure. The presence of hydrophobic interactions emphasizes the high binding affinity of the compound with the receptor protein. Overall, docking results of mutants and WT PTP-1B indicate an increase in the binding affinity of a few compounds including shikonin with the mutant models; however, the binding affinity of most of the compounds was reduced. Close intramolecular interactions responsible for the formation of stable complexes and drug-receptor interactions were significantly reduced when the mutant models were docked with the compounds. It was further confirmed by molecular dynamic simulations, which provide deeper insight into the shikonin and PTP-1B mutants (R24Y, S215E, and S216C) complexes. The MD simulation studies proved that the mutant models did not retain the stable hydrogen bond interaction with the inhibitor compared to the WT PTP-1B and shikonin complex. However, the average binding free energy for shikonin before/after R24Y, S215E, S216C, WT PTP-1B, are -42.407, -41.371, -36.915, -36.175 and -39.221, -29.872, -11.109, -26.55 kcal/mol, respectively, it lost hydrogen bond formation and showed fluctuations throughout the trajectories. The highest energy difference was observed in S216C, and the lowest was observed in R24Y. Furthermore, the binding energy significantly reduced after the course of the trajectory, indicating a significant effect on the inhibitor selectivity of these identified active site residues. The results highlight the importance of the identified active site residues in the formation of a stable inhibitor complex based on the mutation study that reveals reduced binding selectivity upon mutation. Our docking and dynamic simulation result corroborate with the earlier similar findings reported by Yang D. C. et al. Thus, our results suggest that PTP1B active site residues Arg24, Ser215, and Ser216 could play an important role in designing novel and potent PTP1B inhibitors, which could be further developed as therapeutic agents for the management of diabetes.

A combination of evolutionary, intra-molecular interactions and mutational strategies were applied to evaluate the role of identified active site residues from our previous study. The PTP-1B mutant model shares a close structural identity with the wild-type PTP-1B structure. The free binding energy obtained through docking showed significantly low binding energy of the mutant model and shikonin complexes, indicating a lesser binding affinity of shikonin to the mutant model. In WT PTP-1B and the selected compounds, there were more hydrogen bonds, responsible for the stability of the complex, and hydrophobic interactions, which are responsible for the binding affinity. All positions were also investigated structurally and energetically for binding selectivity. The mutant model of R24Y, S215E,

and S216C resulted in relatively unstable binding of shikonin. Results of binding free energy calculations confirmed that the difference in binding affinity is due to R24, S215, and S216. Our findings suggest that, by targeting Arg24, Ser215, and Ser216, potent and selective PTP-1B inhibitors may be designed. These potent inhibitors may further be developed as therapeutic agents for the management of diabetes.

Supplementary Materials
S1 & S2

Ethical Approval & Consent to Participate
Not applicable

Data Availability Statement
The data used to support the findings of this study are included in the article

Competing interests
The authors declare that there is no conflict of interest regarding the publication of this article

Conflicts of Interest
The authors declare no conflict of interest.

References

1. Tonks N K, Protein tyrosine phosphatases--from housekeeping enzymes to master regulators of signal transduction. FEBS J, 2013;280(2):346-78.

2. Elchebly M, Payette P, Michaliszyn E, Cromlish W, Collins S, Loy AL, Normandin D, Cheng A, Himms-Hagen J, Chan CC, Ramachandran C, Gresser MJ, Tremblay ML, Kennedy BP. Increased insulin sensitivity and obesity resistance in mice lacking the protein tyrosine phosphatase-1B gene. Science. 1999 ;283(5407):1544-8. doi: 10.1126/science.283.5407.1544. PMID: 10066179.

3. Koren S, Fantus IG. Inhibition of the protein tyrosine phosphatase PTP1B: potential therapy for obesity, insulin resistance and

type-2 diabetes mellitus. Best Pract Res Clin Endocrinol Metab. 2007; 21(4):621-40. doi: 10.1016/j.beem.2007.08.004. PMID: 18054739.

4. Nguyen PH, Dao TT, Kim J, Phong do T, Ndinteh DT, Mbafor JT, Oh WK. New 5-deoxyflavonoids and their inhibitory effects on protein tyrosine phosphatase 1B (PTP1B) activity. Bioorg Med Chem. 2011; 19(11):3378-83. doi: 10.1016/j.bmc.2011.04.037. Epub 2011 Apr 22. PMID: 21571537.

5. Ye D, Zhang Y, Wang F, Zheng M, Zhang X, Luo X, Shen X, Jiang H, Liu H. Novel thiophene derivatives as PTP1B inhibitors with selectivity and cellular activity. Bioorg Med Chem. 2010;18(5):1773-82. doi: 10.1016/j.bmc.2010.01.055. Epub 2010 Jan 28. PMID: 20153651.

6. Song Z, He XP, Li C, Gao LX, Wang ZX, Tang Y, Xie J, Li J, Chen GR. Preparation of triazole-linked glycosylated α-ketocarboxylic acid derivatives as new PTP1B inhibitors. Carbohydr Res. 2011;346(1):140-5. doi: 10.1016/j.carres.2010.10.023. Epub 2010 Oct 30. PMID: 21111404.

7. Feldhammer M, Uetani N, Miranda-Saavedra D, Tremblay ML. PTP1B: a simple enzyme for a complex world. Crit Rev Biochem Mol Biol. 2013;48(5):430-45. doi: 10.3109/10409238.2013.819830. Epub 2013 Jul 23. PMID: 23879520.

8. Abdelsalam SS, Korashy HM, Zeidan A, Agouni A. The Role of Protein Tyrosine Phosphatase (PTP)-1B in Cardiovascular Disease and Its Interplay with Insulin Resistance. Biomolecules. 2019;9(7):286. doi: 10.3390/biom9070286. PMID: 31319588; PMCID: PMC6680919.

9. Saeed M, Shoaib A, Tasleem M, Alabdallah NM, Alam MJ, Asmar ZE, Jamal QMS, Bardakci F, Alqahtani SS, Ansari IA, Badraoui R. Assessment of Antidiabetic Activity of the Shikonin by Allosteric Inhibition of Protein-Tyrosine Phosphatase 1B (PTP1B) Using State of Art: An In Silico and In Vitro Tactics. Molecules. 2021;26(13):3996. doi: 10.3390/molecules26133996. PMID: 34208908; PMCID: PMC8271486.

10. Chen X, Liu X, Gan Q, Feng C, Zhang Q. Molecular Dynamics Simulations of A27S and K120A Mutated PTP1B Reveals Selective Binding of the Bidentate Inhibitor. Biomed Res Int. 2019;2019:9852897. doi: 10.1155/2019/9852897. PMID: 30729132; PMCID: PMC6341276.

11. Lovering F, Bikker J, Humblet C. Escape from flatland: increasing saturation as an approach to improving clinical success. J Med Chem. 2009;52(21):6752-6. doi: 10.1021/jm901241e. PMID: 19827778.

12. Altschul SF, Gish W, Miller W, Myers EW, Lipman DJ. Basic local alignment search tool. J Mol Biol. 1990;215(3):403-10. doi: 10.1016/S0022-2836(05)80360-2. PMID: 2231712.

13. Sievers F, Wilm A, Dineen D, Gibson TJ, Karplus K, Li W, Lopez R, McWilliam H, Remmert M, Söding J, Thompson JD, Higgins DG. Fast, scalable generation of high-quality protein multiple sequence alignments using Clustal Omega. Mol Syst Biol. 2011;7:539. doi: 10.1038/msb.2011.75. PMID: 21988835; PMCID: PMC3261699.

14. Tiwari MK, Coghi P, Agrawal P, Yadav DK, Yang LJ, Congling Q, Sahal D, Wai Wong VK, Chaudhary S. Novel halogenated arylvinyl-1,2,4 trioxanes as potent antiplasmodial as well as anticancer agents: Synthesis, bioevaluation, structure-activity relationship and in-silico studies. Eur J Med Chem. 2021;224:113685. doi: 10.1016/j.ejmech.2021.113685. PMID: 34303874.

15. Kong X, Sun H, Pan P, Li D, Zhu F, Chang S, Xu L, Li Y, Hou T. How Does the L884P Mutation Confer Resistance to Type-II Inhibitors of JAK2 Kinase: A Comprehensive Molecular Modeling Study. Sci Rep. 2017;7(1):9088. doi: 10.1038/s41598-017-09586-3. PMID: 28831147.

16. Tasleem M, Ishrat R, Ahmad F, Hassan MI, Structural characterization, homology modeling and docking studies of ARG674 Mutation in MyH8 Gene associated with trismus-pseudocamptodactyly syndrome. Lett. Drug Des. Discov. 2014. 11(10):1177-1187.

17. Bernaldez MJ, Billones JB, and Magpantay AE. In silico analysis of binding interactions between GSK983 and human DHODH through docking and molecular dynamics. in AIP Conference Proceedings. 2018. AIP Publishing LLC.

18. Derewenda ZS, Lee L, Derewenda U. The occurrence of C-H...O hydrogen bonds in proteins. J Mol Biol. 1995;252(2):248-62. doi: 10.1006/jmbi.1995.0492. PMID: 7674305.

19. Monzon AM, Zea DJ, Fornasari MS, Saldaño TE, Fernandez-Alberti S, Tosatto SC, Parisi G. Conformational diversity analysis reveals three functional mechanisms in proteins. PLoS Comput Biol. 2017;13(2):e1005398. doi: 10.1371/journal.pcbi.1005398. PMID: 28192432; PMCID: PMC5330503.

20. Damm KL, Carlson HA. Gaussian-weighted RMSD superposition of proteins: a structural comparison for flexible proteins and predicted protein structures. Biophys J. 2006;90(12):4558-73. doi: 10.1529/biophysj.105.066654. Epub 2006 Mar 24. PMID: 16565070; PMCID: PMC1471868.

21. Saini S, Jyoti-Thakur C, Kumar V, Suhag A, Jakhar N. In silico mutational analysis and identification of stability centers in human interleukin-4. Mol Biol Res Commun. 2018;7(2):67-76. doi: 10.22099/mbrc.2018.28855.1310. PMID: 30046620; PMCID: PMC6054777.

22. Ritchie TJ, Macdonald SJ. The impact of aromatic ring count on compound developability--are too many aromatic rings a liability in drug design? Drug Discov Today. 2009;14(21-22):1011-20. doi: 10.1016/j.drudis.2009.07.014. PMID: 19729075.

23. Nittinger E, Inhester T, Bietz S, Meyder A, Schomburg KT, Lange G, Klein R, Rarey M. Large-Scale Analysis of Hydrogen Bond Interaction Patterns in Protein-Ligand Interfaces. J Med Chem. 2017;60(10):4245-4257. doi: 10.1021/acs.jmedchem.7b00101. Epub 2017 May 12. PMID: 28497966.

24. Panigrahi SK, Desiraju GR. Strong and weak hydrogen bonds in the protein-ligand interface. Proteins. 2007;67(1):128-141. doi: 10.1002/prot.21253. PMID: 17206656.

25. Valley CC, Cembran A, Perlmutter JD, Lewis AK, Labello NP, Gao J, Sachs JN. The methionine-aromatic motif plays a unique role in stabilizing protein structure. J Biol Chem. 2012;287(42):34979-34991. doi: 10.1074/jbc.M112.374504. PMID: 22859300; PMCID: PMC3471747.

26. David Ebuka Arthur, Adamu Uzairu, Molecular docking studies on the interaction of NCI anticancer analogues with human Phosphatidylinositol 4,5-bisphosphate 3-kinase catalytic subunit, J. King Saud Univ. Sci.2019; 31(4), 1151-1166.doi.org/10.1016/j.jksus.2019.01.011

27. Castro-Aceituno, Veronica & Siddiqi, Muhammad & Sungeun, Ahn & Natarajan, Sathishkumar & Noh, Hae & Simu, Shakina & Jimenez, Zuly & Yang, Deok-Chun. The Inhibitory Mechanism of Compound K on A549 Lung Cancer Cells through EGF Pathway: An in Silico and in Vitro Approach. Current science. 2016. 111(6). doi: 10.18520/cs/v111/i6/1071-1077.